PHYSICAL REVIEW B **82**, 060518(R) (2010)

London penetration depth in $Ba(Fe_{1-x}T_x)_2As_2$ (T=Co, Ni) superconductors irradiated with heavy ions

H. Kim,[1] R. T. Gordon,[1] M. A. Tanatar,[1] J. Hua,[2] U. Welp,[2] W. K. Kwok,[2] N. Ni,[1] S. L. Bud'ko,[1] P. C. Canfield,[1] A. B. Vorontsov,[3] and R. Prozorov[1,*]

[1]*Ames Laboratory and Department of Physics & Astronomy, Iowa State University, Ames, Iowa 50011, USA*

[2]*Materials Science Division, Argonne National Laboratory, Argonne, Illinois 60439, USA*

[3]*Department of Physics, Montana State University, Bozeman, Montana 59717, USA*

(Received 13 August 2010; published 31 August 2010)

Irradiation with Pb ions was used to study the effect of disorder on the in-plane London penetration depth, $\lambda(T)$, in single crystals of $Ba(Fe_{1-x}T_x)_2As_2$ (T=Co, Ni). An increase in the irradiation dose results in a monotonic decrease in the superconducting transition temperature, T_c, without affecting much the transition width. In both Co- and Ni-doped systems we find a power-law behavior, $\Delta\lambda(T) \propto T^n$ with the exponent n systematically decreasing with the increase in disorder. This observation, at qualitative odds with the response of s- and d-wave superconductors, finds natural explanation in a nodeless $s^{\pm}$ state with pairbreaking (interband) impurity scattering. We are able to describe the effect quantitatively assuming the pairbreaking strength intermediate between Born and unitary limits.

DOI: 10.1103/PhysRevB.82.060518 PACS number(s): 74.70.Xa, 74.25.N−, 74.20.Rp, 74.20.Mn

The mechanism of superconductivity in Fe-based superconductors[1] is a focus of extensive experimental[2] and theoretical[3,4] efforts. Understanding the superconducting gap structure is crucial for identifying the pairing mechanism. While most of the experiments suggest that the general structure of the pairing state belongs to the most symmetric A_{1g} class, the multiband nature of these materials allows for a number of possibilities, including the conventional s-wave state, extended $s^{\pm}$ state with different signs of the order parameter on two bands[4–8] and states with highly anisotropic gaps and even nodes.[9–13]

The London penetration depth can be measured with great precision and its variation with temperature depends sensitively on the gap structure. For $T \leq T_c/3$, a conventional isotropic s-wave gap Δ_0 results in an exponential behavior, $\Delta\lambda(T) \propto \exp(-\Delta_0/T)$, which is preserved even with the addition of nonmagnetic impurities.[14] Unconventional pairing states, on the other hand, are susceptible to the presence of nonmagnetic impurities.[3,8,15–17] In nodal d-wave superconductors, $\lambda(T)$ exhibits a power-law behavior, $\Delta\lambda(T) \propto T^n$ with the exponent n *increasing* from $n=1$ in the clean case to 2 in the dirty limit.[18] For the extended $s^{\pm}$ state, the *opposite* trend is expected: $\Delta\lambda(T)$ is exponential in the clean limit, changing with disorder to a power law, with n as low as 1.6.[15,16]

Experimentally, a power-law behavior with the exponent $2 \leq n < 3$ has been observed in most of the iron-based superconductors.[19–26] This characteristic exponent $n \sim 2$ can be explained in both dirty d-wave and dirty $s^{\pm}$ scenarios. The disorder is always present in the iron-based superconductors where doping (e.g., Co or Ni in this work) is needed to induce superconductivity. One way to resolve this complication is to deliberately introduce defects that do not contribute extra charge but rather only increase the scattering rate. Various ways of controlling the scattering rate have been suggested in earlier studies, especially for the high-T_c cuprates, and the effects have been examined by using transport and magnetic measurements.[27,28] In particular, irradiation with heavy ions, besides producing efficient pinning centers, also significantly enhances scattering, as evident from the significant increase in the normal-state resistivity[29,30] as well as the suppression of T_c.

In this work, we study the in-plane London penetration depth in single crystals of optimally Co- and Ni-doped $BaFe_2As_2$ superconductors irradiated with 1.4 GeV $^{208}Pb^{56+}$ ions. In both systems we find monotonic suppression of T_c with the increase in the irradiation dose without notable transition broadening. The London penetration depth exhibits a power-law behavior, $\Delta\lambda(T) \propto AT^n (2.2 < n < 2.8)$ with the exponent n *decreasing* with the irradiation dose. This observation, qualitatively at odds with the response of s- and d-wave superconductors, provides the most convincing case for the nodeless $s^{\pm}$ state with (interband) pairbreaking scattering.

Single crystals of $Ba(Fe_{1-x}T_x)_2As_2$ (T=Co and Ni denoted FeCo122 and FeNi122, respectively) were grown out of FeAs flux using a high-temperature solution growth technique.[31,32] X-ray diffraction, resistivity, magnetization, and wavelength dispersive spectroscopy elemental analysis have all shown good-quality single crystals at the optimal dopings with a small variation in the dopant concentration over the sample and sharp superconducting transitions, T_c=22.5 K for FeCo122 and 18.9 K for FeNi122.[31,32] The in-plane London penetration depth was measured by using the tunnel diode resonator technique.[33–36] The sample was placed with its crystallographic c axis parallel to a small excitation field, $H_{ac} \approx 20$ mOe. The shift of the resonant frequency, $\Delta f(T)$, is proportional to the sample magnetic susceptibility, $\chi(T)$ via $\Delta f(T) = -G4\pi\chi(T)$. Here G is a geometric calibration factor, $G = f_0 V_s / 2V_c(1-N)$, where N is the demagnetization factor, V_s is the sample volume, and V_c is the coil volume. The calibration factor was determined from the full frequency change by physically pulling the sample out of the coil. The magnetic susceptibility can be written in terms of λ and the characteristic length R, $4\pi\chi = (\lambda/R)\tanh(R/\lambda) - 1$, from which $\Delta\lambda$ can be acquired.[34]

To examine the effect of irradiation, $\sim 2 \times 0.5 \times 0.02 - 0.05$ mm^3 single crystals were selected and then cut

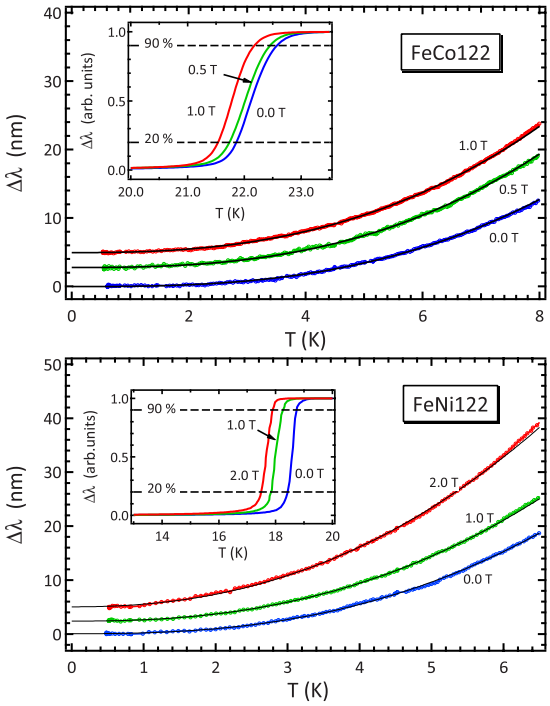

FIG. 1. (Color online) Variation in the in-plane London penetration depth, $\Delta\lambda(T)$, for irradiated FeCo122 (top panel) and FeNi122 (bottom panel). The low-temperature variations are shown in the main frame of each panel along with the best power-law fits. The curves are offset vertically for clarity. The variations in the vicinity of T_c are shown in the insets of each panel.

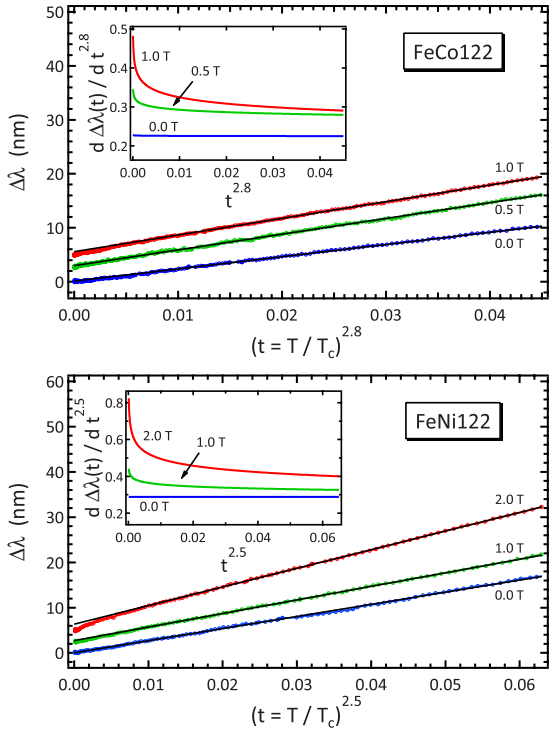

FIG. 2. (Color online) Detailed comparison of the functional form of $\Delta\lambda(T)$ for irradiated FeCo122 and FeNi122. In the main panels $\Delta\lambda(T)$ is plotted vs $(t=T/T_c)^{n_0}$ with the exponents n taken from the best fits of *unirradiated* samples: $n_0=2.8$ and 2.5 for FeCo122 and FeNi122, respectively (see Fig. 1). Apparently, irradiation causes low-temperature deviations, which are better seen in the derivatives, $d\Delta\lambda(t)/dt^{n_0}$, plotted in the insets.

into several pieces preserving the width and the thickness. We compare sets of samples, where the samples in each set are parts of the same original large crystal and had identical temperature-dependent penetration depth in unirradiated state. Several such sets were prepared and a reference piece was kept unirradiated from each set. Irradiation with 1.4 GeV $^{208}Pb^{56+}$ ions was performed at the Argonne Tandem Linear Accelerator System (ATLAS) with an ion flux of $\sim 5\times 10^{11}$ ions s^{-1} m^{-2}. The actual total dose was recorded in each run. The density of defects (d) created by the irradiation is usually expressed in terms of the matching field, $B_\phi=\Phi_0 d$, which is obtained assuming one flux quanta, $\Phi_0 \approx 2.07\times 10^{-7}$ G cm^2 per ion track. Here we studied samples with $B_\phi=0.5$, 1.0, and 2.0 T corresponding to $d=2.4\times 10^{10}$, 4.8×10^{10}, and 9.7×10^{10} cm^{-2}. The sample thickness was chosen in the range of $\sim 20-50$ μm to be smaller than the ion penetration depth, 60–70 μm. The same samples were studied by magneto-optical imaging.[37] The strong Meissner screening and large uniform enhancement of pinning have shown that the irradiation has produced uniformly distributed defects.[37]

Figure 1 shows $\Delta\lambda(T)$ for FeCo122 (top panel) and FeNi122 (bottom panel). The low-temperature region up to $\approx T_c/3$ is shown in the main frame of each panel. Vertical offsets were applied for clarity. The normalized penetration depths in the vicinity of T_c are shown in the inset of each panel to highlight the suppression of T_c as the radiation dose increases. Whereas T_c is clearly suppressed, the transition width remains nearly the same (see Fig. 3). All samples exhibit a power-law variation in $\Delta\lambda(T)\propto T^n$ with $2.5<n<2.8$ up to $T_c/3$ while the exponential fitting failed in all cases. We note that we see no signature of an upturn caused by paramagnetic effects[23] hence we conclude that the defects induced by the irradiation are not magnetic. The exponent n and its error bar were determined by fitting over several temperature ranges as described in Ref. 26. The best fitting curves are shown by solid lines in Fig. 1. We note that the present set of FeCo122 samples exhibits higher exponents, n, compared to previous works.[20,25] This variation in n is likely due to chemical variation between different batches. Consequently, it is important to conduct a comparison of radiation effects on the samples made from the *same* large crystal. Magneto-optical characterization has shown a homogeneous superconducting response[37] and the widths of the superconducting transitions were much smaller than the absolute shift due to irradiation, see Fig. 3. Therefore, it is very likely that the effects reported here are caused by the enhanced scattering induced by the heavy-ion bombardment.

To further analyze the power-law behavior and its variation with irradiation, we plot $\Delta\lambda$ as a function of $(t=T/T_c)^{n_0}$ in Fig. 2, where the n_0 values for FeCo122 and FeNi122 were chosen from the best power-law fits of the unirradiated samples (see Fig. 3). While the data for unirradiated samples appear as almost perfect straight lines showing robust power-law behavior, the curves for irradiated samples show downturns at low temperatures indicating

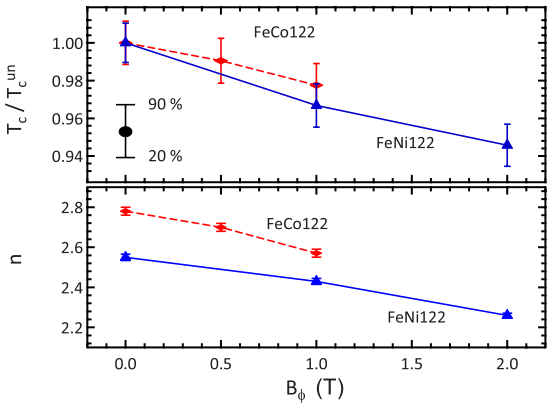

FIG. 3. (Color online) Top panel: the suppression of T_c with disorder relative to *unirradiated* T_c^{un}. The vertical bars denote the width of the transition corresponding the diamagnetic signal change from 90% (onset) to 20% (end), see insets in Fig. 1. Symbols are shown at the mean values between onset and end of the transition. Lower panel: exponent n vs B_ϕ.

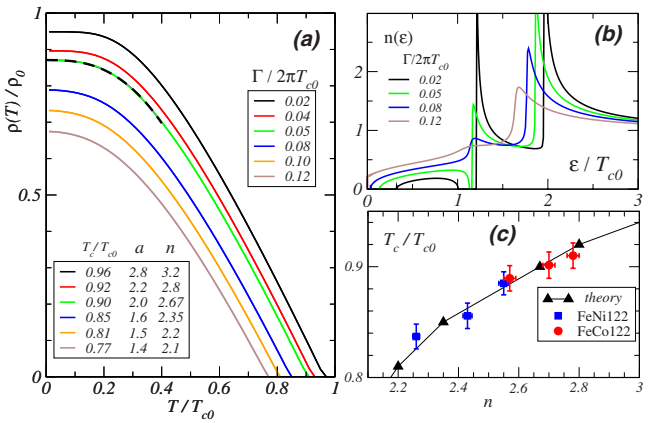

FIG. 4. (Color online) (a) Superfluid density and (b) the density of states $n(\varepsilon)=N(\varepsilon)/N_f$, computed for the $s^\pm$ state with sign-changing isotropic gaps and strong interband impurity scattering, between the Born and unitary limits. The dashed line in (a) is an example of a power-law fit $\rho(T)/\rho_0=\rho(0)/\rho_0-a(T/T_{c0})^n$ for $0<T<0.4T_{c0}$; best fitting parameters for a given set of $\Gamma=n_{imp}/\pi N_f$ are listed in the table. (b) As the impurity concentration $n_{imp}\sim\Gamma$ increases, the band of midgap states approaches the Fermi level and the exponent n is reduced. (c) T_c vs power n, from the theoretical model (triangles) and experiment (squares and circles).

smaller exponents. This observation, emphasized by the plots of the derivatives $d\Delta\lambda(t)/dt^{n_0}$ in the inset of Fig. 2, points to a significant change in the low-energy excitations with radiation.

The variations in T_c and n upon irradiation are illustrated in Fig. 3. Dashed lines and circles show FeCo122 while solid lines and triangles show FeNi122. The upper panel shows the variation in T_c and the width of the transition. Since B_ϕ is directly proportional to the area density of the ions, d, we can say that T_c decreases roughly linearly with d. The same trend is evident for the exponent n shown in the lower panel of Fig. 3. The fitting prefactor A increases somewhat upon the increase in irradiation dose but remains smaller than the value measured previously in unirradiated samples.[19,20,25]

The experimental results fit comfortably within the hypothesis of $s^\pm$ superconductivity with two isotropic gaps. The superfluid density in linear response is

$$\rho(T) = \sum_{i=1,2} \pi T \sum_{\varepsilon_m} N_{f,i} \int_{FS_i} d\hat{\mathbf{p}} [\mathbf{v}_{f,i} \otimes \mathbf{v}_{f,i}]_{xx} \frac{\tilde{\Delta}_i^2}{(\tilde{\varepsilon}_m^2 + \tilde{\Delta}_i^2)^{3/2}}, \quad (1)$$

where one sums over the contributions from the electron and hole bands; $\mathbf{v}_{f,i}$ and $N_{f,i}$ are the Fermi velocity and density of states in these bands, taken to be equal for the calculations. Two order parameters $\Delta_{1,2}$ are computed self-consistently together with the t-matrix treatment of impurity effects, which renormalize the Matsubara energies $i\tilde{\varepsilon}_m=i\varepsilon_m-\Sigma_{imp,i}$ and the gaps $\tilde{\Delta}_i=\Delta_i+\Delta_{imp,i}$.[38] Impurities are characterized by the strength of the potential for scattering within each band, $v_{11}(=v_{22})$, given by the phase shift $\delta=\tan^{-1}(\pi N_f v_{11})$, the ratio of potentials for interband and intraband hopping, $\delta v=v_{12}/v_{11}$, and the impurity scattering rate $\Gamma=n_{imp}/\pi N_f$.

The essential theoretical results are presented in Fig. 4 while the full calculations will be published elsewhere.[39] The best agreement with the experiment is obtained for two isotropic gaps, $\Delta_2\approx-0.6\Delta_1$, strong interband scattering $\delta v=0.9$ and phase shift $\delta=60°$ between the Born ($\delta\to0$) and unitary limits ($\delta\to90°$). The calculated $\rho(T)$ was fitted to the power law, $\rho(T)/\rho_0\approx\rho(0)/\rho_0-a(T/T_{c0})^n$, which is directly related to the penetration depth, $\Delta\lambda(T)/\lambda_0\approx a'(T/T_c)^n$ with ρ_0 and λ_0 being the $T=0$ superfluid density and penetration depth in the clean system and $a'=(a/2)[T_c/T_{c0}]^n[\rho_0/\rho(0)]^{3/2}$. We find that with an increase in Γ, the power n decreases from $n\gtrsim3$ to $n\approx2$ [see Fig. 4(a)], which is in perfect agreement with experiment. The values of n depend *sensitively* on the structure of the low-energy density of states, which is shown in Fig. 4(b). The intermediate strength of scatterers is important for creation of a *small* band of midgap states separated from the continuum. As the disorder is increased, these states close the gap in the spectrum and gradually increase in magnitude, driving the low-temperature power-law dependence from exponential-like, $n>3$, to $n\approx2$. This behavior of n is largely independent of the details of the model, whereas a' can slightly increase or decrease depending on the different ratios of the gaps on two Fermi surfaces and different impurity parameters.

Finally, in Fig. 4(c) we show the central result of our study: the correlation between T_c and n. Note that these two quantities are obtained essentially independently of each other. Assuming that the unirradiated samples have some disorder due to doping, and scaling T_c^{un} to lie on the theoretical curve, we find that the $T_c(B_\phi)$ of the irradiated samples also follows this curve. The assumption of similarity between doping and radiation-induced disorder, implied in this comparison while not unreasonable, deserves further scrutiny.

In summary, we determined the effect of irradiation on $\lambda(T)$ and demonstrated that the disorder-induced reduction in the power-law exponent $2<n<3$ is naturally explained in terms of the isotropic extended s-wave state[3,4] with pair-

breaking interband scattering.[3,17,40] We have also considered models for nodal states, but they showed the opposite trends: increase in n with disorder in the interval $1 < n \leqslant 2$, and thus can be excluded. Taken together with reports of fully gapped states from thermal conductivity,[41] angle-resolved photoemission spectroscopy[42] and phase-sensitive Josephson-junction measurements,[43] our results present a convincing case, in favor of the extended $s^{\pm}$ pairing symmetry having a nodeless order parameter in the optimally doped 122 system.

The picture of strong pair-breaking scattering is also consistent with recent proposals of the universal behavior in the thermal and electromagnetic responses of iron-based superconductors.[17,44,45] Nonetheless, we should note that nodal states may still exist in P-containing compounds[46–48] or along the c axis of heavily overdoped Ba122 pnictides.[24]

We thank V. Kogan, J. Schmalian, A. Chubukov, I. Mazin, P. Hirschfeld, and A. Koshelev for useful discussions. This work was supported by the U.S. Department of Energy, Office of Basic Energy Sciences, Division of Materials Sciences and Engineering under Contract No. DE-AC02-07CH11358 (Ames National Laboratory) and Contract No. DE-AC02-06CH11357 (Argonne National Laboratory). The heavy-ion irradiation was performed at the ATLAS facility at Argonne. R.P. acknowledges support from the Alfred P. Sloan Foundation.

*Corresponding author; prozorov@ameslab.gov

[1] Y. Kamihara *et al.*, J. Am. Chem. Soc. **130**, 3296 (2008).
[2] K. Ishida *et al.*, J. Phys. Soc. Jpn. **78**, 062001 (2009).
[3] A. V. Chubukov, Physica C **469**, 640 (2009).
[4] I. I. Mazin and J. Schmalian, Physica C **469**, 614 (2009).
[5] I. I. Mazin, D. J. Singh, M. D. Johannes, and M. H. Du, Phys. Rev. Lett. **101**, 057003 (2008).
[6] K. Kuroki, S. Onari, R. Arita, H. Usui, Y. Tanaka, H. Kontani, and H. Aoki, Phys. Rev. Lett. **101**, 087004 (2008).
[7] V. Barzykin and L. P. Gorkov, JETP Lett. **88**, 131 (2008).
[8] V. Cvetkovic and Z. Tesanovic, EPL **85**, 37002 (2009).
[9] K. Seo, B. A. Bernevig, and J. Hu, Phys. Rev. Lett. **101**, 206404 (2008).
[10] T. A. Maier, S. Graser, D. J. Scalapino, and P. J. Hirschfeld, Phys. Rev. B **79**, 224510 (2009).
[11] S. Graser *et al.*, New J. Phys. **11**, 025016 (2009).
[12] A. V. Chubukov, M. G. Vavilov, and A. B. Vorontsov, Phys. Rev. B **80**, 140515(R) (2009).
[13] R. Thomale, C. Platt, J. Hu, C. Honerkamp, and B. A. Bernevig, Phys. Rev. B **80**, 180505(R) (2009).
[14] M. Tinkham, *Introduction to Superconductivity* (Dover, New York, 1996).
[15] Y. Bang, EPL **86**, 47001 (2009).
[16] A. B. Vorontsov, M. G. Vavilov, and A. V. Chubukov, Phys. Rev. B **79**, 140507 (2009).
[17] R. T. Gordon, H. Kim, M. A. Tanatar, R. Prozorov, and V. G. Kogan, Phys. Rev. B **81**, 180501(R) (2010).
[18] P. J. Hirschfeld and N. Goldenfeld, Phys. Rev. B **48**, 4219 (1993).
[19] R. T. Gordon *et al.*, Phys. Rev. Lett. **102**, 127004 (2009).
[20] R. T. Gordon, C. Martin, H. Kim, N. Ni, M. A. Tanatar, J. Schmalian, I. I. Mazin, S. L. Bud'ko, P. C. Canfield, and R. Prozorov, Phys. Rev. B **79**, 100506(R) (2009).
[21] K. Hashimoto *et al.*, Phys. Rev. Lett. **102**, 207001 (2009).
[22] C. Martin *et al.*, Phys. Rev. B **80**, 020501(R) (2009).
[23] C. Martin *et al.*, Phys. Rev. Lett. **102**, 247002 (2009).
[24] C. Martin, H. Kim, R. T. Gordon, N. Ni, V. G. Kogan, S. L. Bud'ko, P. C. Canfield, M. A. Tanatar, and R. Prozorov, Phys. Rev. B **81**, 060505(R) (2010).
[25] L. Luan, O. M. Auslaender, T. M. Lippman, C. W. Hicks, B. Kalisky, J. H. Chu, J. G. Analytis, I. R. Fisher, J. R. Kirtley, and K. A. Moler, Phys. Rev. B **81**, 100501(R) (2010).
[26] H. Kim *et al.*, Phys. Rev. B **81**, 180503(R) (2010).
[27] *Processing and Properties of High-T_c Superconductors*, edited by S. Jin (World Scientific, Singapore, 1993).
[28] G. Blatter *et al.*, Rev. Mod. Phys. **66**, 1125 (1994).
[29] Y. Zhu, Z. X. Cai, R. C. Budhani, M. Suenaga, and D. O. Welch, Phys. Rev. B **48**, 6436 (1993).
[30] S. I. Woods, A. S. Katz, M. C. deAndrade, J. Herrmann, M. B. Maple, and R. C. Dynes, Phys. Rev. B **58**, 8800 (1998).
[31] P. C. Canfield, S. L. Bud'ko, N. Ni, J. Q. Yan, and A. Kracher, Phys. Rev. B **80**, 060501(R) (2009).
[32] N. Ni, M. E. Tillman, J. Q. Yan, A. Kracher, S. T. Hannahs, S. L. Bud'ko, and P. C. Canfield, Phys. Rev. B **78**, 214515 (2008).
[33] C. T. Van Degrift, Rev. Sci. Instrum. **46**, 599 (1975).
[34] R. Prozorov, R. W. Giannetta, A. Carrington, and F. M. Araujo-Moreira, Phys. Rev. B **62**, 115 (2000).
[35] R. Prozorov *et al.*, Appl. Phys. Lett. **77**, 4202 (2000).
[36] R. Prozorov and R. W. Giannetta, Supercond. Sci. Technol. **19**, R41 (2006).
[37] R. Prozorov, M. A. Tanatar, B. Roy, N. Ni, S. L. Bud'ko, P. C. Canfield, J. Hua, U. Welp, and W. K. Kwok, Phys. Rev. B **81**, 094509 (2010).
[38] V. Mishra, A. Vorontsov, P. J. Hirschfeld, and I. Vekhter, Phys. Rev. B **80**, 224525 (2009).
[39] A. B. Vorontsov (unpublished).
[40] A. Glatz and A. E. Koshelev, Phys. Rev. B **82**, 012507 (2010).
[41] M. A. Tanatar, J. P. Reid, H. Shakeripour, X. G. Luo, N. Doiron-Leyraud, N. Ni, S. L. Bud'ko, P. C. Canfield, R. Prozorov, and L. Taillefer, Phys. Rev. Lett. **104**, 067002 (2010).
[42] K. Terashima *et al.*, Proc. Natl. Acad. Sci. U.S.A. **106**, 7330 (2009).
[43] X. Zhang, Y. S. Oh, Y. Liu, L. Yan, K. H. Kim, R. L. Greene, and I. Takeuchi, Phys. Rev. Lett. **102**, 147002 (2009).
[44] S. L. Bud'ko, N. Ni, and P. C. Canfield, Phys. Rev. B **79**, 220516(R) (2009).
[45] V. G. Kogan, Phys. Rev. B **81**, 184528 (2010).
[46] J. D. Fletcher, A. Serafin, L. Malone, J. G. Analytis, J. H. Chu, A. S. Erickson, I. R. Fisher, and A. Carrington, Phys. Rev. Lett. **102**, 147001 (2009).
[47] C. W. Hicks, T. M. Lippman, M. E. Huber, J. G. Analytis, J. H. Chu, A. S. Erickson, I. R. Fisher, and K. A. Moler, Phys. Rev. Lett. **103**, 127003 (2009).
[48] H. Shishido *et al.*, Phys. Rev. Lett. **104**, 057008 (2010).